



Deposited via The University of Leeds.

White Rose Research Online URL for this paper:

<https://eprints.whiterose.ac.uk/id/eprint/85202/>

Version: Accepted Version

Article:

Harbottle, D, Chen, Q, Moorthy, K et al. (2014) Problematic Stabilizing Films in Petroleum Emulsions: Shear Rheological Response of Viscoelastic Asphaltene Films and the Effect on Drop Coalescence. *Langmuir*, 30 (23). pp. 6730-6738. ISSN: 0743-7463

<https://doi.org/10.1021/la5012764>

Reuse

Items deposited in White Rose Research Online are protected by copyright, with all rights reserved unless indicated otherwise. They may be downloaded and/or printed for private study, or other acts as permitted by national copyright laws. The publisher or other rights holders may allow further reproduction and re-use of the full text version. This is indicated by the licence information on the White Rose Research Online record for the item.

Takedown

If you consider content in White Rose Research Online to be in breach of UK law, please notify us by emailing eprints@whiterose.ac.uk including the URL of the record and the reason for the withdrawal request.

Problematic stabilizing films in petroleum emulsions: shear rheological response of viscoelastic asphaltene films and the effect on drop coalescence

David Harbottle^{1*}, Qian Chen², Krishna Moorthy¹, Louxiang Wang¹, Shengming Xu², Qingxia Liu¹, Johan Sjoblom³ and Zhenghe Xu^{1,2*}

Corresponding Authors: Zhenghe.xu@ualberta.ca and harbottl@ualberta.ca

¹ Department of Chemical and Materials Engineering, University of Alberta, Edmonton, Alberta, Canada, T6G2V4.

² Institute of Nuclear and New Energy Technology, Tsinghua University, P.R. China, 100084.

³ Ugelstad Laboratory, Department of Chemical Engineering, Norwegian University of Science and Technology (NTNU), Trondheim, Norway.

Abstract

Adsorption of asphaltenes at the water-oil interface contributes to the stability of petroleum emulsions by forming a networked film that can hinder drop-drop coalescence. The interfacial microstructure can either be liquid-like or solid-like, depending on: i) initial bulk concentration of asphaltenes, ii) interfacial aging time, and iii) solvent aromaticity. Two techniques: interfacial shear rheology and integrated thin film drainage apparatus provided equivalent interface aging conditions, enabling direct correlation of the interfacial rheology and droplet stability. The shear rheological properties of the asphaltene film were found to be critical to the stability of

contacting droplets. With a viscous dominant interfacial microstructure, the coalescence time for two drops in intimate contact was rapid, on the order of seconds. However, as the elastic contribution develops and the film microstructure begins to be dominated by elasticity, the two drops in contact do not coalesce. Such step-change transition in coalescence is thought to be related to the high shear yield stress ($\sim 10^4$ Pa), which is a function of the film shear yield point and the film thickness (as measured by quartz crystal microbalance), and the increased elastic stiffness of the film that prevents mobility and rupture of the asphaltene film which when in a solid-like state provides an energy barrier for the droplets to coalesce.

Keywords: asphaltenes, interfacial shear rheology, drop coalescence, yield stress, film thickness

Introduction

As world demand for energy continues to increase the production rate of conventional and unconventional oil will follow the demand. The process of efficient oil extraction and recovery raises many scientific challenges that have long been considered. One particular area that continues to receive much attention is the rapid and efficient separation of water and oil in the produced fluids from oil reserves. With all production methods, the creation of problematic emulsions is often unfortunately unavoidable.

Crude oil and bitumen are composed of a variety of chemical species that are often subcategorized into saturates, aromatics, resins and asphaltenes (SARA).¹ Of those compounds both resins and asphaltenes have been discussed as fractions that affect emulsion stability and hence oil-water separation.^{2, 3, 4, 5, 6, 7} While resins are often considered surfactant-like, the complexity of asphaltenes has resulted in a definition described by a solubility class, with no

analogous system from which similarities can be drawn. Competitive interaction of those species at the water-oil interface has been considered by several researchers,^{3, 8, 9, 10} while the introduction of resins has been shown to soften or increase the flexibility of an asphaltene interfacial film.^{3, 11}

When studying micron-sized water drops immersed in diluted bitumen, Wu¹² considered the response of interfacial films to drop volume reduction. At low (solvent:bitumen) dilution ratio, the drop shape was maintained during withdrawal of water, while at high dilution ratio, the interfacial material offered resistance to in-plane shear as observed by drop crumpling. Analysis of the interfacial material showed that such resistance results from the accumulation of asphaltenes. This research clearly demonstrated the formation of an “armored” film surrounding a drop acting as a barrier to drop coalescence, similar to that frequently observed in Pickering and Colloidosome droplet emulsions.^{13, 14}

The mechanism for drop stabilization in the presence of resins, asphaltenes or mixed component systems is different; however asphaltenes have received significant attention due to their role in the formation of extremely stable layers often referred to as ‘dense-packed’ or ‘rag-layers’ . In the worst case the presence of this densely packed layer can completely stop the oil-water separation process.^{6, 15}

The rheological study of interfacial asphaltene films by harmonic volume oscillations of a pendant drop has shown that the dilatational elasticity dominates the interfacial microstructure with only a small viscous contribution.^{16, 17, 18} Such rheological characteristic has been observed over a wide range of asphaltene concentrations and extensive aging time, with emulsion stability at equivalent asphaltene concentrations being qualitatively linked to rheological properties of the

interfacial film. It is interesting to note and will be discussed further in the paper that for unbuffered systems the time dependence of the interfacial film on the dilatational rheology is almost negligible over an extended aging period.¹⁶

A second deformation mode of the interfacial material can be described as the deformation by shear applied to a constant interfacial area, as opposed to the variable area as encountered during the dilatation.¹⁹ Kilpatrick and co-workers reinvigorated interest in the shear rheological response of petroleum films.^{20, 21} Applying the bicone technique, the authors conducted an extensive study on the interfacial films of asphaltenes extracted from different crude oils. They concluded that asphaltenes of lower aromaticity and higher nitrogen and metal contents form stable emulsion as a result of film aging which increases yield stress as measured under shear. In higher aliphatic solvents the onset of asphaltene precipitation was observed to delay film formation and the development of microstructure elasticity. Below the onset of precipitation, film aging kinetics increased closer to the solubility limit.²⁰ Possibly due to the inertial contribution of the bicone, the authors did not report any effect of aging at relatively short aging time, < 2 hr.

Fan and co-workers²² used the same bicone technique to study film aging kinetics of asphaltenes dispersed in toluene-heptane (6:4) solution. After 20 hr of aging, the frequency dependent rheological properties of the interfacial film indicated the formation of a consolidated network, with both the viscous and elastic response of the film exhibiting a small dependency on oscillation frequency. Through the addition of chemical demulsifiers to the asphaltene solution, the authors reported only a viscous component with no measurable elasticity over 20 hr of film aging. The absence of an elastic contribution is potentially due to the occupancy of interfacial

area by highly surface active demulsifier molecules, preventing the adsorption of asphaltene molecules.

Research to date has largely compared the interfacial rheological response, both dilatation and shear, to emulsion stability measured by bottle tests. However, there are two significant differences between the two approaches: i) the surface area to volume ratio of the rheology and emulsion stability (bottle tests) experiments is substantially different; and ii) the aging mechanism in the two approaches is different, i.e. in the case of rheology the interfacial film is formed by diffusion-controlled adsorption, while the vigorous mixing in the formation of an emulsion introduces an advection term that is not well controlled. Those differences have potentially limited our progression when trying to determine critical conditions for drop and emulsion stability. In the present study, the surface area to volume ratio for both rheology measurement and drop stability (coalescence) test using our newly designed interfacial force balance is almost equivalent and the mechanism for asphaltene film formation for both cases is governed by diffusion-controlled adsorption. Such an approach allows for comparison of the two data sets so that the direct link between interfacial rheology and emulsion stability can be established with great confidence.

Materials and Experimental Methods

Materials: *Asphaltene precipitation* – the C5 asphaltene fraction was precipitated from Athabasca bitumen that was kindly provided by Syncrude Canada Ltd. Extended details on the extraction method are provided in the Supporting Documentation Section 1.

Solution preparation – in the current study the effect of two different solvents, toluene and heptol 1:1 (heptane/toluene, v/v), and two different asphaltene concentrations, 0.1 and 0.4 g/L, were considered. All organic solvents were obtained from Fisher Scientific (Canada) and used in this study without further purification. Further guidance on the solution preparation method is provided in the Supporting Document Section 2.

Aqueous phase – all water used throughout the study was deionized Milli-Q[®] grade with a conductivity of approximately $\sim 0.05 \mu\text{Scm}^{-1}$. The pH of the aqueous phase was unadjusted at pH 5.5.

Experimental Methods: *Integrated Thin Film Drainage Apparatus (ITFDA)* – a unique feature of the present study was the use of a custom-built ITFDA to measure the real drop-drop coalescence time. Figure 1a shows a schematic of the instrumentation and liquid cell. Details on the instrument set-up and capabilities have been provided in reference.²³ Details specific to the current experimental program can be found in the Supporting Document Section 3.

A typical bimorph output from the ITFDA during a drop-drop coalescence event is shown in Figure 1b. Initially, the drops are held apart for up to 6 hr at a separation distance of 0.55 mm, $t = 0$ s. After a desired aging period, the drop fixed on the capillary was lowered towards the second drop, with the displacement and rate of approach controlled by a computer activated speaker diaphragm. In the current study, the total capillary displacement was set to 670 μm providing an apparent drop-drop overlap of 120 μm , thus ensuring that the drops were in intimate contact, and the approach time was equal to 1 s. With the displacement of the glass capillary, the two drops begin to interact as evidenced by the increased bimorph voltage at $t = 0.91$ s. A positive voltage corresponds to a downward displacement of the bimorph from the initial

position. With the two drops in contact the bimorph signal remains steady at ~ 0.03 V, until at $t = 11.96$ s after initial drop displacement, the bimorph signal suddenly jumps to -0.85 V. The dramatic shift in the bimorph signal results from the coalescence of the two drops, permitting accurate measurement of the time between drop-drop contact and coalescence. In the example shown, the coalescence time is $t = 11.05$ s. Calibration of the bimorph beam deflection by the addition of known masses resulted in a constant of 16.12 V/mN. Based on this calibration and the voltage response at drop-drop contact (Figure 1b), the applied interaction force is equal to ~ 1.9 μ N. For all experiments the interaction force varied in the range 1.2 and 2.5 μ N.

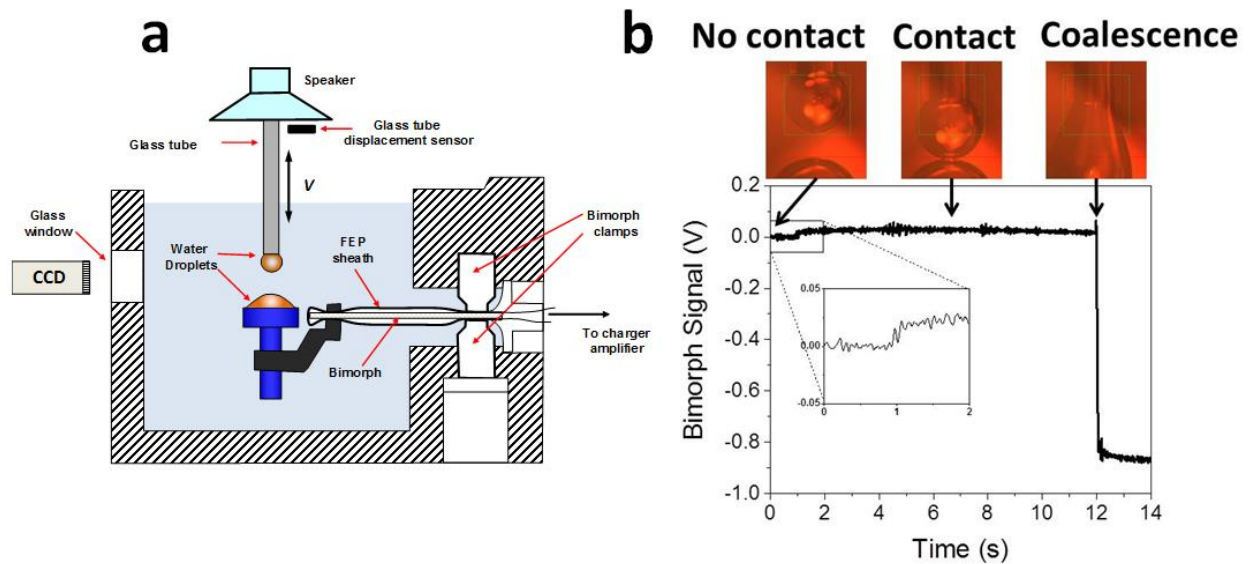


Figure 1 a) Schematic of the integrated thin film drainage apparatus used to determine the real drop-drop coalescence time. b) Raw data of the bimorph signal as two water drops partially stabilized by an asphaltene film are moved and held in contact until coalescence.

Interfacial rheology using Double Wall Ring (DWR) geometry – an AR-G2 controlled stress rheometer (TA Instruments, Canada) with double wall ring (DWR) geometry²⁴ was used to measure the viscoelasticity and shear yield stress of asphaltene-stabilized films. The DWR geometry is used in combination with a circular channel Delrin[®] trough. To pin the liquid-liquid

interface the channel is machined with a lip at 10 mm above the channel base. The cross-section length of the radial channel is 8.5 mm. The DWR geometry has a diagonal cross-section length of 1 mm, with a square-edge to pin the interface. The geometry is flamed prior to use to ensure the removal of organic matter or other contaminants that may accumulate on the surface. Before each measurement the inertia and rotational mapping of the instrument were calibrated. To maximize the sensitivity of the instrument, precision mapping was chosen with the transducer bearing mode set to soft. The Delrin[®] trough was fixed directly onto the AR-G2 Peltier plate that was maintained at 23°C. First, 19.2 mL water was pipetted into the trough so that the liquid-liquid interface above the channel base was maintained at approximately ~12,000 μm. Second, using the instrument software (Trios v2.6.2) the ring was lowered to 20,000 μm gap, followed by manual positioning of the ring at the air-water interface. Third, 18 mL of the organic phase was gently pipetted onto the sub-phase, placing the fluid onto the inner wall of the trough to prevent disruption of the interface. A Teflon cap was then placed over the trough to minimize evaporation and any atmospheric disturbances.

Preliminary experiments during interfacial aging were conducted to identify the region of linear viscoelasticity. For an angular frequency of 0.5 Hz, 0.8% strain was shown to be within the linear viscoelastic region. The oscillatory conditions for a time sweep were fixed at 0.5 Hz and 0.8% strain, with data points collected periodically for 4.5 hr.

After film aging, an oscillation amplitude sweep was applied to measure the film yield stress. By increasing the oscillatory stress (1×10^{-5} to 0.01 N/m), the integral nature of the film begins to break down, represented by a sharp decrease in G' . The intersection of two linear regions, before and after film rupture, was used to determine the critical yield stress of the film. Further details

on the interfacial rheology measurement and the associated theory can be found in the Supporting Document Section 4.

Quartz crystal microbalance with dissipation monitoring – the microbalance technique was used to measure asphaltene adsorption and layer formation (thickness) on a solid substrate (gold coated piezo-electric crystal). Experiments were completed to determine the apparent asphaltene layer thickness based on appropriate modeling of the frequency and dissipation data. Prior to each measurement the sensor (5MHz, gold-coated quartz crystal) was sonicated for 10 min in ethanol, rinsed with Milli-Q[®] water, dried with dry nitrogen and cleaned further with UV irradiation ($\sim 9 \text{ mW cm}^{-2}$ at 254 nm) for at least 10 min. Finally, the crystal was rinsed once again with Milli-Q[®] water and dried with dry nitrogen. The sensor was then mounted into the Q-Sense E4 flow module (Q-Sense, Sweden) and the overtone peaks determined to assess the cleanliness of the sensor. The sensor resonant frequency and dissipation was first stabilized in air for 15 min at 23°C, followed by an air-solvent transition, either toluene or heptol 1:1. The solvent was then pumped through the measurement cell for 5 min to form a stable baseline. With a stable frequency and dissipation response, the asphaltene solution was pumped into the measurement cell at a flow rate of 14 $\mu\text{L}/\text{min}$. The flow rate was maintained for 4.5 hr with the frequency and dissipation of the resonating sensor continually measured as the asphaltene film develops on the sensor surface. For all the QCM-D experiments the crystal drive amplitude was fixed at 0.4 a.u.. Theory and background associated with the QCM-D measurement can be found in Section 5 of the Supporting Document.

Results and Discussion

Drop-drop coalescence time – the coalescence time determined from the bimorph trace, for two aged water drops in contact is shown in Figure 2a. The data shows the coalescence time to be a

function of: i) aging time, ii) solvent aromaticity and iii) asphaltene concentration. Considering the data for all aging times from 5 min to 6 hr, there appears to be a step-change transition in the drop coalescence time, with the critical transition time dependent on experimental conditions. This step-change transition is clearly observed for the case of two water drops aged in 0.4 g/L asphaltene in heptol 1:1. After 30 min of drop aging the average coalescence time from 10 measurements was ~ 7.5 s, as shown in Figure 2b. With an additional 30 min aging (total 1 hr) the average coalescence time increased to ~ 23 s, with a higher variability as shown by the associated uncertainty. To improve confidence in the experimental data 10 repeat experiments were completed for the fast (in seconds) coalescing drops. The increase in coalescence time from 7.5 s to 23 s supports the understanding that asphaltenes in solution adsorb to the water-oil interface, forming an interfacial barrier that hinders drop coalescence. However, with an additional 1 hr of aging (total 2 hr) the coalescence time was greater than 900 s. With the coalescence time greater than 900 s the drops were considered stable to coalescence and hence the exact coalescence time was not measured. It is evident that with one additional hour of aging the coalescence time increased from the order of seconds to no coalescence. Similar behavior was also observed for the three additional experimental conditions. In the case of 0.4 g/L asphaltene in toluene, the average drop coalescence time after 5 min aging was less than 2 s, indicating little resistance to drainage and film rupture. After 30 min aging the coalescence time increased to ~ 3.8 s and then ~ 16.8 s after 2 hr aging, as shown in Figure 2b. After 4 hr of aging the interacting drops no longer coalesce within 900 s and were considered stable. A similar trend over 4 hr aging was observed for 0.1 g/L asphaltene in heptol 1:1. However, for 0.1 g/L asphaltene in toluene the drop coalescence time remained low, ~ 5.1 s after 2 hr of aging. With a further 4 hr of aging (total 6 hr) the two drops were shown to coalesce at an extended time of 670

s. Even though the drops were aged for an additional 2 hr compared with all other experimental conditions, the system remained unstable (exhibits a coalescence time less than 900 s). The time to reach the condition of no coalescence increased in the order of 0.4 g/L asphaltene in heptol 1:1 < 0.4 g/L asphaltene in toluene \approx 0.1 g/L asphaltene in heptol 1:1 < 0.1 g/L asphaltene in toluene. These results clearly illustrate the critical role of solvent aromaticity and asphaltenes concentration in influencing the stability of emulsion droplets.

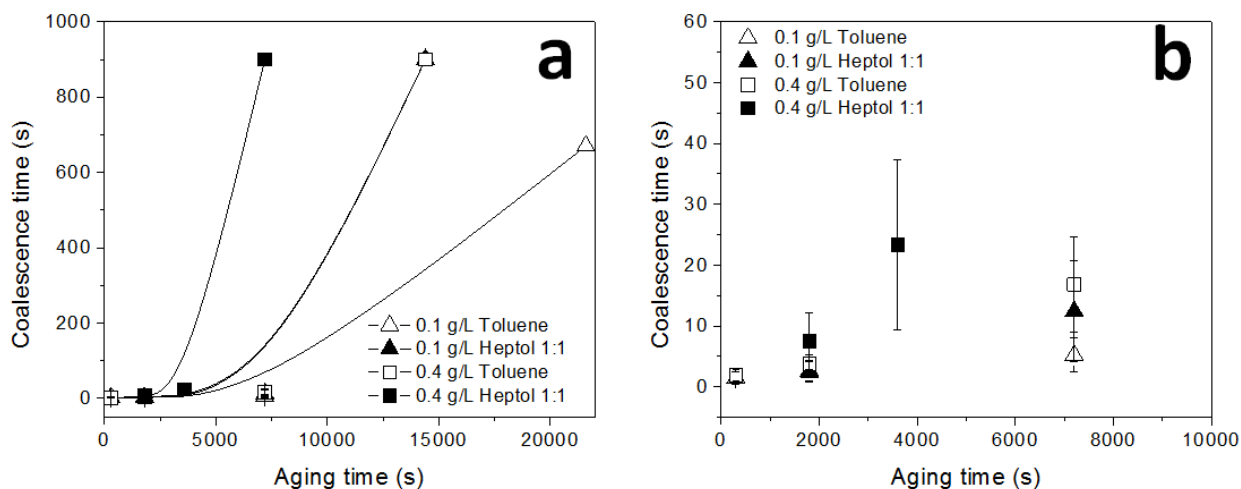


Figure 2 a) Coalescence time for water drops aged in asphaltene solutions of varying asphaltene concentration and solvent aromaticity, b) Expanded region showing the coalescence behavior at short aging times.

The solubility of asphaltenes is shifted at different heptane/toluene ratio, with all of the asphaltenes insoluble in heptane and all of the asphaltenes soluble in toluene. Whilst remaining below the condition for asphaltene precipitation, the change in solubility would influence the interfacial activity of asphaltene molecules. Yarranton and Hussien²⁵ showed the interfacial activity of asphaltenes to be inversely related to solubility by changing the attractive potential between asphaltene structural heteroatoms and water. In a good solvent (toluene), the attraction

between the solvent molecules and asphaltene molecules is strong as indicated by their high solubility, reducing the interfacial activity of asphaltene molecules. While in a poor solvent (heptol, 1:1), the interaction between the asphaltene molecule and the solvent molecules is weak, resulting in an increase in interfacial activity of asphaltene molecules.

The effect of solvent aromaticity (aromatic/aliphatic ratio) on asphaltene interfacial activity qualitatively supports the coalescence time data with drop aging (Figure 2a). For an equivalent asphaltene concentration, the change in drop coalescence time with interfacial aging is faster when the asphaltenes are dispersed in a poor solvent. While interfacial activity and the accumulation of asphaltenes at the water-oil interface describes the increased coalescence time with drop aging, the mechanism that governs the step-change in drop coalescence time from the order of seconds to no coalescence with aging time remains to be established.

Interfacial rheology – the shear rheology of an asphaltene interfacial film (asphaltene adsorption and structuring at the water-oil interface) was studied by oscillation measurement. The viscoelastic properties (G' and G'') of the interfacial film were periodically measured for 4.5 hr. Figure 3a shows the viscoelastic aging characteristics of an interfacial film formed from 0.1 g/L asphaltene in either toluene (square symbols) or heptol 1:1 (circle symbols). If we first consider the case of 0.1 g/L asphaltene in toluene, at $t = 0$ s the film was purely viscous with a modulus in the range of 4.5×10^{-5} N/m. The viscous response remains steady around this value for almost 1 hr before exhibiting a small growth throughout the remainder of the experiment. At 4.3 hr towards the end of the experiment, the onset of an elastic modulus $> 1 \times 10^{-5}$ N/m was measured, although the film remains viscous dominant. When measuring the film aging characteristics in heptol 1:1 (0.1 g/L asphaltene), the initial condition was equivalent to that in toluene. However, the viscous modulus begins to develop almost immediately and the early detection of an elastic

modulus was shown after ~ 1.3 hr. While the viscous modulus continues to develop, the linear growth in the elastic contribution is faster, leading to a transition condition from liquid-like to solid-like, elastic dominant microstructure. In the case of 0.1 g/L asphaltene in heptol 1:1, the condition $G' = G''$ was satisfied at $t = 2.64$ hr.

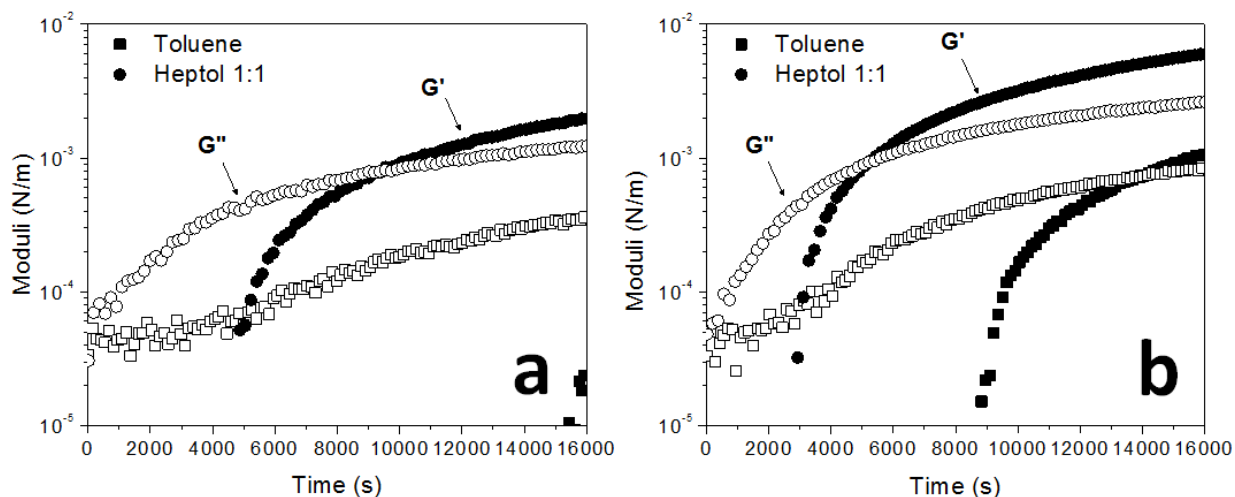


Figure 3 Time dependent viscoelastic (G' and G'') properties of asphaltene films. a) 0.1 g/L asphaltenes, b) 0.4 g/L asphaltenes dispersed in either toluene or heptol 1:1. Experimental conditions: strain 0.8%, frequency 0.5 Hz, temperature 23°C.

For 0.4 g/L asphaltene in either toluene or heptol 1:1, viscoelastic aging of the film shows the same trend as the low concentration samples, with a much faster film aging in heptol 1:1 than in toluene. The condition $G' = G''$ was satisfied at 3.87 hr and 1.45 hr for 0.4 g/L asphaltene in toluene and heptol 1:1, respectively. A comparison of all four interfacial aging profiles (G' vs. G'') is shown in Figure 4. In general, the formation of interfacial film as measured by viscoelasticity is similar, although there are small differences that may be related to the effect of solvent aromaticity on asphaltene aggregation. Comparing the two 0.4 g/L asphaltene samples, at short aging time the development in both G' and G'' is identical up to $G' \approx 1.2 \times 10^{-4}$ N/m.

With continued film development the two aging profiles begin to deviate. For an equivalent G'' , the corresponding G' was lower for the sample prepared in heptol 1:1 as compared with the sample in toluene. G'' can be considered a good indicator of asphaltene accumulation, as shown by 0.1 g/L asphaltene in toluene, where $G'' \uparrow$ and $G'' \approx 0$ N/m, and G' can be considered a good indicator of asphaltene film cross-linking.²² Based on this interpretation of the two viscoelastic properties, deviation of the two aging profiles may result from strong interaction and cross-linking between asphaltenes within the interfacial film.

Formation of the interfacial film is most likely influenced by the interaction forces between asphaltenes in solution that can be pseudo-quantitatively understood by an interaction parameter,²⁶ $\chi = V_{heptol}(\delta_{asph} - \delta_{heptol})^2/RT$, where V_{heptol} is the molar volume of the solvent heptol (m^3/mol), δ_{asph} and δ_{heptol} are the Hildebrand solubility parameters of asphaltenes and heptol, respectively ($\text{MPa}^{1/2}$), T is the temperature (K), and R is the universal gas constant ($J/ \text{mol } K$). Using the Hildebrand solubility parameters provided in literature for asphaltenes ($20 \text{ MPa}^{1/2}$), heptane ($15.3 \text{ MPa}^{1/2}$) and toluene ($18.3 \text{ MPa}^{1/2}$),²⁶ and calculating the Hildebrand solubility parameter of heptol 1:1 on a volume average basis and the molar volume of heptol 1:1 calculated on a molar average basis, χ in heptol 1:1 and toluene is equal to 0.52 and 0.13, respectively. A smaller χ would represent an increased miscibility of the asphaltenes with the solvent, while a higher χ would represent decreased miscibility between the asphaltenes and solvent, favoring aggregation of asphaltene molecules. When the asphaltenes are well solvated they can arrange and pack more tightly within the interfacial film, conversely nano-aggregates and/or nano-clusters of asphaltenes will interact to form open porous networks. Such behavior is also supported by film thickness measurements reported later in this article. The close packing in a miscible environment may support a higher G' contribution for an equivalent G'' when

compared to a system of decreased miscibility, see Figure 4. Such interpretation of the interaction potential and the effect on elasticity is in agreement with observations in particle suspensions.²⁷ It is also interesting to note that below $G' = 1.2 \times 10^{-4}$ N/m (Figure 4) the viscoelastic development in the interfacial film is independent of solvent aromaticity. Such behavior may support the understanding that the interfacial film initially forms through the adsorption of asphaltene molecules²⁸ followed by slower diffusing aggregates and nano-clusters in poor solvents.²⁹

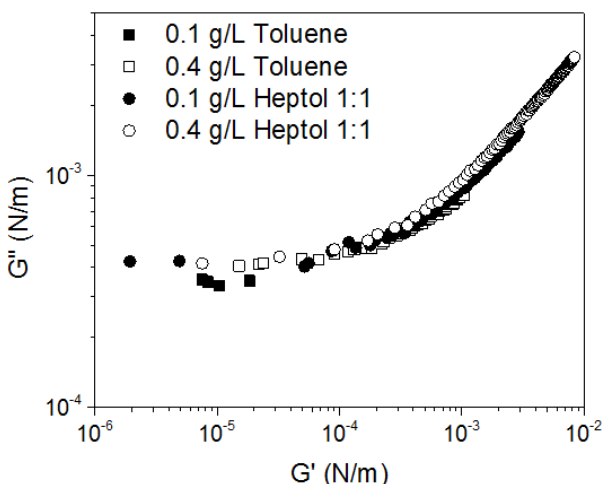


Figure 4 Characteristic interfacial aging profiles of asphaltene films formed in toluene and heptol 1:1.

Interfacial rheology and drop stability – the experimental program was carefully designed to minimize differences between the two data sets; interfacial rheology and drop coalescence. For almost equivalent surface area to volume ratios, film formation was governed by diffusion-controlled adsorption and subsequent reorganization of the interfacial molecules in the absence of advection diffusion. For this reason, the two data sets can be directly compared. For 0.4 g/L asphaltene in heptol 1:1, the initial film microstructure is predominantly viscous and corresponds to short drop coalescence times on the order of seconds. Beyond the condition, $G' = G''$, the

interfacial microstructure is predominantly elastic and the interacting drops do not coalesce. This behavior in drop coalescence time was consistent for all experimental conditions, as shown in Figure 5.

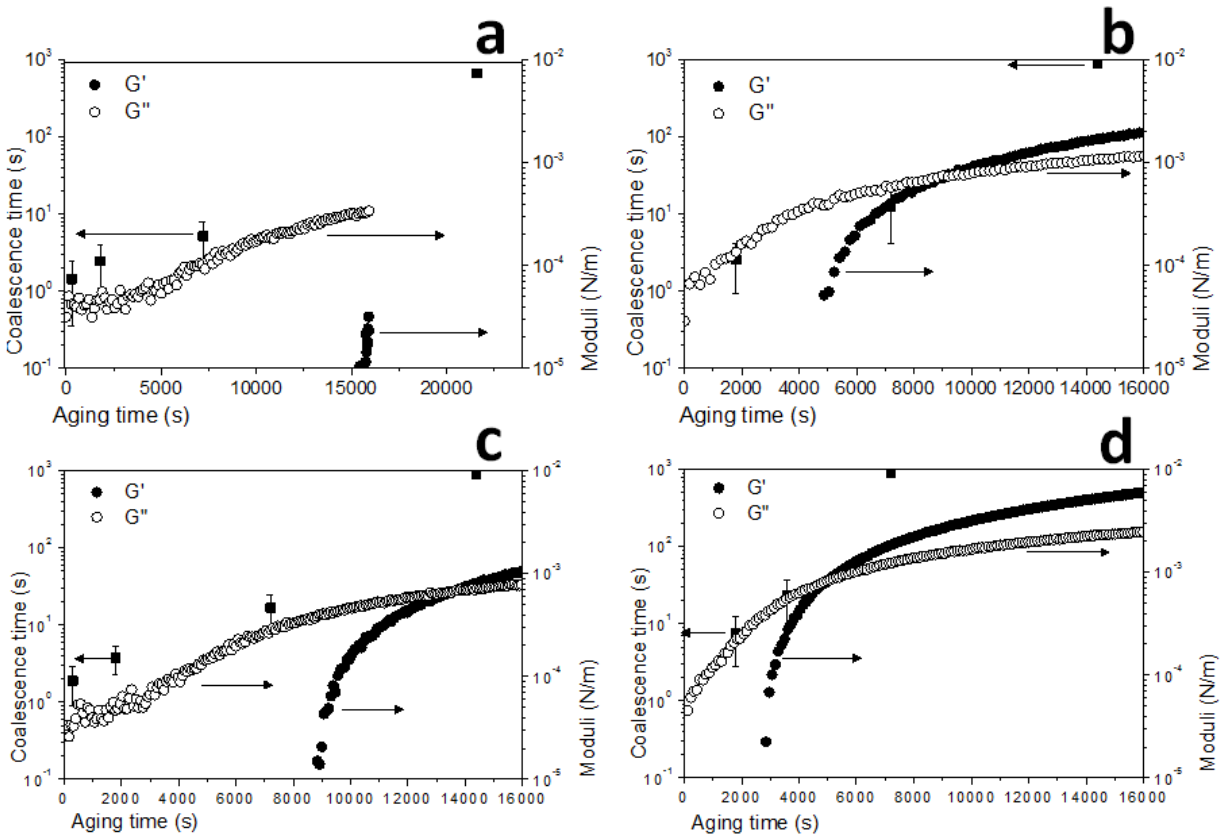


Figure 5 Direct comparisons of interfacial viscoelastic properties and drop-drop coalescence time as a function of aging time. a) 0.1 g/L asphaltene in toluene, b) 0.1 g/L asphaltene in heptol 1:1, c) 0.4 g/L asphaltene in toluene and d) 0.4 g/L asphaltene in heptol 1:1.

Adsorption of asphaltenes at the water-oil interface has been studied by several researchers with the mechanism for film formation debated in the literature.^{21, 28} The more accepted understanding is that asphaltene films form over two characteristic time scales of aging: i) diffusion and ii) relaxation, with the second phase controlled mainly by asphaltene rearrangement within the

film.^{20, 30} Asphaltene molecules in close proximity can form a variety of intermolecular bridges by π - π interaction of the aromatic core, hydrogen bonds, charge-transfer interactions, multi-polar force, and van der Waals interactions.² Clear identification of these two characteristic times of aging from shear rheology data is nontrivial. Measuring the G' and G'' contribution of an asphaltene film (initial condition 0.4 g/L asphaltene in heptol 1:1, see Figure 6), the viscoelastic response would support a long characteristic time for film rearrangement as shown by the continual and extensive growth in the G' contribution, while G'' plateaus after ~ 29 hr of interfacial aging. Continual accumulation and cross-linking of asphaltene molecules will affect the cohesive energy density or strength of the interfacial film. For the long aging time experiment shown in Figure 6, 1 mL of heptol 1:1 was gently pipetted onto the top phase every 8 hr to minimize any effect from solvent loss.

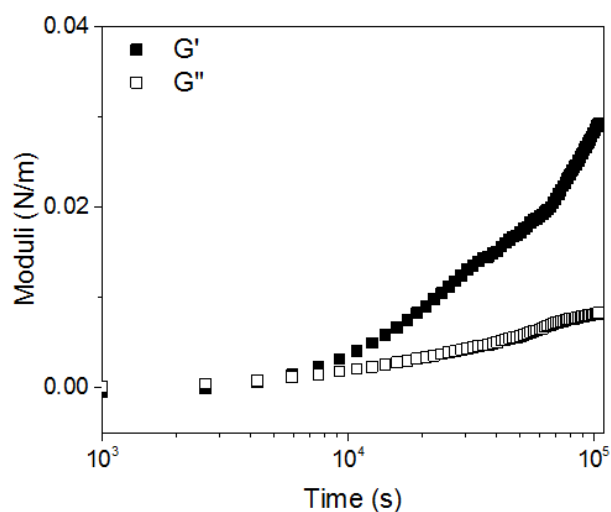


Figure 6 Long time development in the viscoelasticity of an asphaltene film, initial condition: 0.4 g/L asphaltene in heptol 1:1. Experimental conditions: strain 0.8%, frequency 0.5 Hz, temperature 23°C.

Interfacial film yield stress – the yield point of an aged interfacial film was measured by an amplitude sweep completed at the end of each experiment. For the three films that resulted in an elastic dominant microstructure, Figure 7 shows the G' and G'' dependence on oscillation stress. At low oscillation stress, G' and G'' remain constant indicating that the response is within the linear viscoelastic region. At a critical oscillation stress, G' decreases rapidly while G'' increases slightly, followed by a gradual decrease. The slight increase in G'' for those films that are strongly elastic has been reported previously and is believed to result from the creation of pieces of film that contribute to the viscous stress as the structural integrity of the film is broken.²⁰ The rapid decrease and eventual disappearance of the G' component also indicate that the interfacial film microstructure has yielded. The yield point has been determined from the intersection of two linear fits; i) linear viscoelastic region and ii) non-linear viscoelastic region.

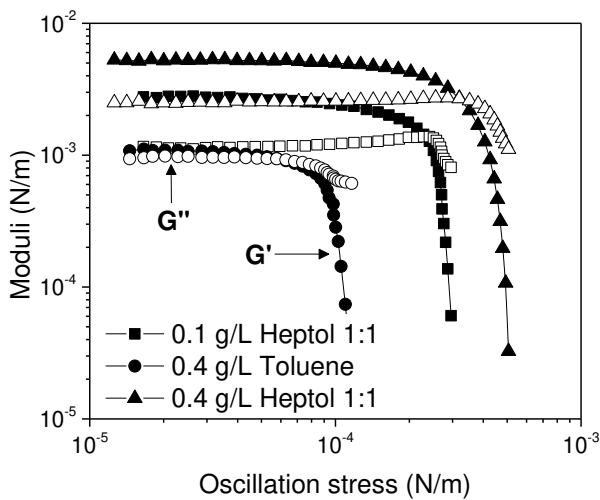


Figure 7 Oscillation stress sweep conducted on aged ($t = 4.5$ hr) asphaltene films.

Table 1 shows an increase in the interfacial film yield point with increasing asphaltene concentration and aliphatic to aromatic solvent ratio (column 2). When measuring the film

rheology the physical properties are two-dimensional hence, the yield point is reported as N/m and not N/m^2 . To determine the apparent yield stress the film thickness should be considered.³¹

Table 1 Comparison of the two-dimensional yield point and the apparent asphaltene film yield stress at $t = 4.5$ hr aging. * Asphaltene film thickness measured by QCM-D.

Sample	Yield point (N/m)	Apparent yield stress* (N/m^2)
0.4 g/L asphaltene in toluene	9.26×10^{-5}	9.9×10^3
0.1 g/L asphaltene in heptol 1:1	2.50×10^{-4}	1.6×10^4
0.4 g/L asphaltene in heptol 1:1	4.17×10^{-4}	9.8×10^3

Film thickness – measuring the dynamic film thickness at a liquid-liquid interface is nontrivial. However, a reasonable approximation can be made from the measurement of film thickness at a solid-liquid interface, provided that the solid surface is highly hydrophilic to retain a thin layer of water molecules of anchored hydroxyl groups. Using QCM-D, the film thickness can be determined from appropriate modeling of frequency (Sauerbrey) and/or frequency and dissipation (Voigt) data. In good solvent (toluene) the resonant frequency and dissipation shifts of the 5th overtone after 4.5 hr were: $\Delta f = -38.8$ Hz and $\Delta D = 1.3 \times 10^{-6}$, and $\Delta f = -52.8$ Hz and $\Delta D = 3.4 \times 10^{-6}$ for asphaltene concentrations of 0.1 g/L and 0.4 g/L, respectively (data not shown). Based on the Sauerbrey approximation the thickness of the asphaltene film in toluene is 6.9 nm (0.1 g/L asphaltene) and 9.3 nm (0.4 g/L asphaltene) as shown in Figure 8. Those values are in good agreement with film thickness measurements by surface forces apparatus.³² For asphaltenes dispersed in heptol 1:1 the frequency and dissipation shifts at equivalent concentrations were larger; $\Delta f = -84.0$ Hz and $\Delta D = 4.8 \times 10^{-6}$ for 0.1 g/L asphaltenes in heptol 1:1; and $\Delta f = -221.7$ Hz and $\Delta D = 19.8 \times 10^{-6}$ for 0.4 g/L asphaltenes in heptol 1:1. Modeling the data by Sauerbrey (S) and Voigt (V) approach, the film thickness after 4.5 hr aging was

determined to be 13.8 nm (S) and 15.5 nm (V), and 35.0 (S) nm and 41.8 nm (V) for asphaltene concentrations of 0.1 g/L and 0.4 g/L, respectively. A slightly thinner film calculated by Sauerbrey results from treating the film as a rigid layer. The viscoelastic modeling is in agreement with the interfacial rheology data which showed significant development in both the viscous and elastic properties of interfacial films formed in heptol 1:1. To enable modeling of the film thickness from frequency and dissipation data an estimate of the layer density is required. In the current study a layer density of 1050 kg/m^3 was used in all cases. Although we did not determine the asphaltene layer density, we did conduct a sensitivity analysis which showed a variation of the film thickness on the order of $\sim 20\%$ when the layer density was varied between 1200 kg/m^3 and 900 kg/m^3 .³³ The values of the asphaltene layer composition and hence the layer density used in our sensitivity analysis are similar to those reported by Verruto and Kilpatrick.³⁴

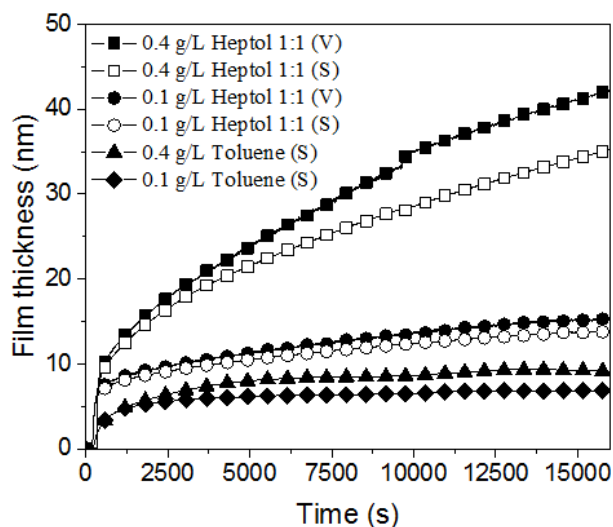


Figure 8 Asphaltene film thicknesses at the solid-liquid interface as measured by QCM-D. Film thickness determined by Sauerbrey (S) or Voigt (V) approximations.

Based on the measured film thickness the apparent yield stress for each asphaltene film is in the range of $1 \times 10^4 \text{ N/m}^2$, see column 3 of Table 1. Using the ITFDA it is possible to measure a

contact force (μN) and contact length (μm) between two interacting drops. With a typical contact force of $2.5 \mu\text{N}$ (drop area change in contact $< 1.0 \%$) and contact length $350 \mu\text{m}$, the interaction stress is equal to $\sim 25 \text{ N/m}^2$ which is considerably lower than the critical stress required to break the cohesive film surrounding a water drop and initiate coalescence. A contact force greater than $\sim 1\text{mN}$ (based on a contact length of $350 \mu\text{m}$) would be required to break the asphaltene microstructure surrounding water drops. It should be noted that with the apparent yield stress calculated from two independent measurement techniques (yield point and film thickness), a slight uncertainty in one value can lead to an observable change in the overall apparent yield stress. For example, a 1 nm uncertainty in the film thickness measurement can lead to a change in the calculated yield stress by approximately 10% for water drops dispersed in 0.4 g/L asphaltene in toluene solution. Based on our findings, we can consider the measured apparent yield stresses approximately equal within uncertainty.

Interfacial film elastic stiffness – the ratio of the viscoelastic moduli may also impact drop coalescence, more specifically the elastic stiffness contribution of the interfacial film. With interfacial aging the interfacial film is observed to transition from liquid-like to solid-like state with the transition time dependent on asphaltene concentration and solvent aromaticity.

The relevance of elastic stiffness may be better understood when considering the effect on the stability of an intervening liquid film (organic phase) as two drops are brought into contact. As the separation distance between the two drops is decreased, instabilities from hydrodynamic and surfaces forces (at a very small separation distance) can result in perturbations that eventually lead to intervening film rupture.³⁵ However, when the interfacial film (asphaltene layer) is predominantly elastic, the destabilizing force can be suppressed to the point where the intervening liquid film drains and the contacting drop interfaces remain stable by the immobility

of the asphaltene layer.³⁶ The stabilizing potential of a viscoelastic thin film to perturbations has been shown to depend on a critical interaction stiffness, $-hY_c/\mu$, where h is the film thickness, μ is the elastic shear modulus and Y_c is the instability potential.³⁷ If the elastic stiffness of the film is greater than the destabilizing interaction stiffness the film will remain stable to perturbations. For viscous dominant films when the elastic contribution is zero the film is unstable to perturbations regardless of the magnitude of the instability force, hence conditions for coalescence are favorable.³⁷

Shear and dilatational rheology – finally we address both the shear and dilatational rheological response of asphaltene films formed in toluene environment of increasing asphaltene concentration, shown in Figure 9. As discussed in the Introduction, much interest has centered on the dilatational rheology of asphaltene films. In general, the link between dilatational rheology and emulsion stability is at best qualitative, with reasonable agreement between increasing dilatational elasticity and emulsion stability. In dilatation the film aging is dominated by elasticity, with the interfacial microstructure upon asphaltene adsorption and rearrangement predominantly elastic even at short aging time of ~10 min. With extended aging the film remains elastic with a small increase in the dilatational elasticity and an almost unchanged dilatational viscosity, as shown in Figure 9. Such behavior is in contrast with the shear response of the asphaltene film. In shear the viscoelastic properties exhibit greater sensitivity to film growth, with both the elastic and viscous properties showing substantial development with film aging. At short aging time, the interfacial microstructure of the asphaltene film as measured by shear is dominated by the viscous contribution. With aging, the elastic contribution develops to form a film with a predominately elastic microstructure. Gradual development of the asphaltene film as measured by shear rheology corresponds well with increased coalescence time and eventual

stable drop-drop condition (as shown in Figure 2). The characteristic aging of asphaltene films as measured by dilatational and shear rheology would indicate that the shear response of the film is more sensitive to drop coalescence.

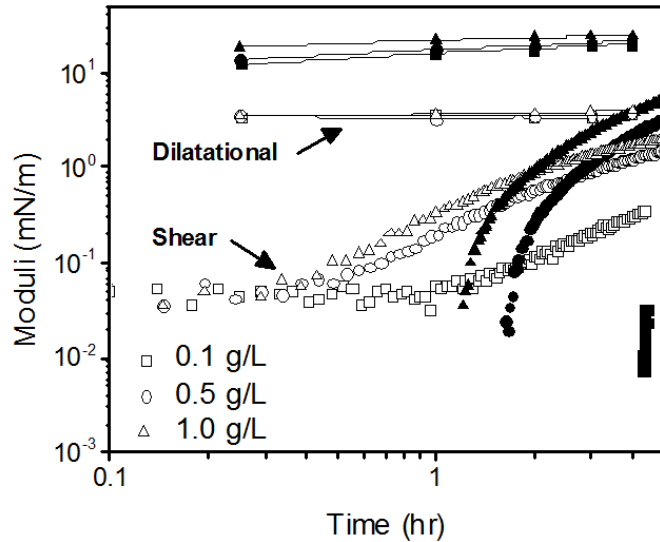


Figure 9 Comparison of the shear and dilatational viscoelastic rheology of aged asphaltene films. Closed symbols: G' ; Open Symbols: G'' .

Conclusions

The drop coalescence time of two water drops dispersed in solvent containing asphaltenes and the shear rheology of the associated liquid-liquid interfacial film has been studied using an integrated thin film drainage apparatus and double wall ring geometry, respectively. The two techniques provide an almost equivalent surface area to volume ratio and allow film formation through diffusion-controlled adsorption and rearrangement. The results from both techniques have been directly compared to show rapid drop coalescence (in seconds) when the film microstructure is dominated by the viscous component, and no coalescence when the interfacial microstructure transitions to a solid-like state and the elastic contribution dominates. The

mechanism by which drop coalescence is prevented is believed to relate to: i) the high shear yield stress of the asphaltene film, in the order of $\sim 10^4$ Pa, formed by the gradual accumulation and rearrangement of asphaltene molecules within the film, and ii) the increasing elastic film stiffness that presents an energy barrier to film instabilities when in the solid-like state.

Comparison of shear and dilatation rheology has shown contrasting behavior. While shear rheology measures a progressive transition in the asphaltene film properties from liquid-like to solid-like behavior, the dilatational response is dominated by elasticity which governs the film rheology at short aging time (in minutes). Unlike shear rheology, dilatation shows minimal aging variability and is therefore difficult to interpret based on the observed changes in drop coalescence.

The study has also shown a significant contact force is required to overcome the apparent shear yield stress of the cohesive asphaltene film surrounding water drops. Such a high interaction force can be overcome by reversing the development of asphaltene film to a liquid-like state, possibly through the addition of chemical demulsifiers that compete for interfacial area and weaken the elastic contribution of the film.

Acknowledgements

The financial support for this work from NSERC (Natural Sciences and Engineering Research Council of Canada) Industrial Research Chair in Oil Sands Engineering is gratefully acknowledged.

Supporting Information

Further details on experimental techniques and methods are provided in the Supporting Document. This information is available free of charge via the Internet at <http://pubs.acs.org/>.

References

1. Graham, B. F.; May, E. F.; Trengove, R. D. Emulsion inhibiting components in crude oils. *Energy & Fuels* **2008**, *22* (2), 1093-1099.
2. Kilpatrick, P. K. Water-in-Crude Oil Emulsion Stabilization: Review and Unanswered Questions. *Energy & Fuels* **2012**, *26* (7), 4017-4026.
3. Yang, X.; Verruto, V. J.; Kilpatrick, P. K. Dynamic asphaltene-resin exchange at the oil/water interface: Time-dependent W/O emulsion stability for asphaltene/resin model oils. *Energy & Fuels* **2007**, *21* (3), 1343-1349.
4. Yan, Z. L.; Elliott, J. A. W.; Masliyah, J. H. Roles of various bitumen components in the stability of water-in-diluted-bitumen emulsions. *Journal of Colloid and Interface Science* **1999**, *220* (2), 329-337.
5. Goual, L.; Horvath-Szabo, G.; Masliyah, J. H.; Xu, Z. H. Adsorption of bituminous components at oil/water interfaces investigated by quartz crystal microbalance: Implications to the stability of water-in-oil emulsions. *Langmuir* **2005**, *21* (18), 8278-8289.
6. Kiran, S. K.; Acosta, E. J.; Moran, K. Study of Solvent-Bitumen-Water Rag Layers. *Energy & Fuels* **2009**, *23*, 3139-3149.
7. Maia, D. C.; Ramalho, J.; Lucas, G. M. S.; Lucas, E. F. Aging of water-in-crude oil emulsions: Effect on rheological parameters. *Colloids and Surfaces a-Physicochemical and Engineering Aspects* **2012**, *405*, 73-78.

8. Zhu, Y.-w.; Zhao, R.-h.; Jin, Z.-q.; Zhang, L.; Zhang, L.; Luo, L.; Zhao, S. Influence of Crude Oil Fractions on Interfacial Tension of Alkylbenzene Sulfonate Solutions. *Energy & Fuels* **2013**, *27* (8), 4648-4653.
9. Neuville, M.; Rondelez, F.; Cagna, A.; Sanchez, M. Two-Step Adsorption of Endogenous Asphaltenic Surfactants at the Bitumen-Water Interface. *Energy & Fuels* **2012**, *26* (12), 7236-7242.
10. Maia Filho, D. C.; Ramalho, J. B. V. S.; Spinelli, L. S.; Lucas, E. F. Aging of water-in-crude oil emulsions: Effect on water content, droplet size distribution, dynamic viscosity and stability. *Colloids and Surfaces a-Physicochemical and Engineering Aspects* **2012**, *396*, 208-212.
11. Kiran, S. K.; Ng, S.; Acosta, E. J. Impact of Asphaltenes and Naphthenic Amphiphiles on the Phase Behavior of Solvent-Bitumen-Water Systems. *Energy & Fuels* **2011**, *25* (5), 2223-2231.
12. Wu, X. Investigating the stability mechanism of water-in-diluted bitumen emulsions through isolation and characterization of the stabilizing materials at the interface. *Energy & Fuels* **2003**, *17* (1), 179-190.
13. Asekomhe, S. O.; Chiang, R.; Masliyah, J. H.; Elliott, J. A. W. Some observations on the contraction behavior of a water-in-oil drop with attached solids. *Industrial & Engineering Chemistry Research* **2005**, *44* (5), 1241-1249.
14. Thompson, K. L.; Giakoumatos, E. C.; Ata, S.; Webber, G. B.; Armes, S. P.; Wanless, E. J. Direct Observation of Giant Pickering Emulsion and Colloidosome Droplet Interaction and Stability. *Langmuir* **2012**, *28* (48), 16501-16511.

15. Khatri, N. L.; Andrade, J.; Baydak, E. N.; Yarranton, H. W. Emulsion layer growth in continuous oil-water separation. *Colloid Surf. A-Physicochem. Eng. Asp.* **2011**, *384* (1-3), 630-642.
16. Yarranton, H. W.; Sztukowski, D. M.; Urrutia, P. Effect of interfacial rheology on model emulsion coalescence - I. Interfacial rheology. *Journal of Colloid and Interface Science* **2007**, *310* (1), 246-252.
17. Sztukowski, D. M.; Yarranton, H. W. Rheology of asphaltene - Toluene/water interfaces. *Langmuir* **2005**, *21* (25), 11651-11658.
18. Alvarez, G.; Poteau, S.; Argillier, J.-F.; Langevin, D.; Salager, J.-L. Heavy Oil-Water Interfacial Properties and Emulsion Stability: Influence of Dilution. *Energy & Fuels* **2009**, *23* (1), 294-299.
19. Erni, P. Deformation modes of complex fluid interfaces. *Soft Matter* **2011**, *7* (17), 7586-7600.
20. Spiecker, P. M.; Kilpatrick, P. K. Interfacial rheology of petroleum asphaltenes at the oil-water interface. *Langmuir* **2004**, *20* (10), 4022-4032.
21. Verruto, V. J.; Le, R. K.; Kilpatrick, P. K. Adsorption and Molecular Rearrangement of Amphoteric Species at Oil-Water Interfaces. *J. Phys. Chem. B* **2009**, *113* (42), 13788-13799.
22. Fan, Y.; Simon, S.; Sjoblom, J. Interfacial shear rheology of asphaltenes at oil-water interface and its relation to emulsion stability: Influence of concentration, solvent aromaticity and nonionic surfactant. *Colloid Surf. A-Physicochem. Eng. Asp.* **2010**, *366* (1-3), 120-128.
23. Wang, L.; Sharp, D.; Masliyah, J.; Xu, Z. Measurement of Interactions between Solid Particles, Liquid Droplets, and/or Gas Bubbles in a Liquid using an Integrated Thin Film Drainage Apparatus. *Langmuir* **2013**, *29* (11), 3594-3603.

24. Vandebril, S.; Franck, A.; Fuller, G. G.; Moldenaers, P.; Vermant, J. A double wall-ring geometry for interfacial shear rheometry. *Rheologica Acta* **2010**, *49*, 131-144.
25. Yarranton, H. W.; Hussein, H.; Masliyah, J. H. Water-in-hydrocarbon emulsions stabilized by asphaltenes at low concentrations. *Journal of Colloid and Interface Science* **2000**, *228* (1), 52-63.
26. Wang, S.; Liu, J.; Zhang, L.; Masliyah, J.; Xu, Z. Interaction Forces between Asphaltene Surfaces in Organic Solvents. *Langmuir* **2010**, *26* (1), 183-190.
27. Grant, M. C.; Russel, W. B. VOLUME-FRACTION DEPENDENCE OF ELASTIC-MODULI AND TRANSITION-TEMPERATURES FOR COLLOIDAL SILICA-GELS. *Physical Review E* **1993**, *47* (4), 2606-2614.
28. Rane, J. P.; Harbottle, D.; Pauchard, V.; Couzis, A.; Banerjee, S. Adsorption Kinetics of Asphaltenes at the Oil-Water Interface and Nanoaggregation in the Bulk. *Langmuir* **2012**, *28* (26), 9986-9995.
29. Natarajan, A.; Xie, J.; Wang, S.; Liu, Q.; Masliyah, J.; Zeng, H.; Xu, Z. Understanding Molecular Interactions of Asphaltenes in Organic Solvents Using a Surface Force Apparatus. *Journal of Physical Chemistry C* **2011**, *115* (32), 16043-16051.
30. Freer, E. M.; Radke, C. J. Relaxation of asphaltenes at the toluene/water interface: Diffusion exchange and surface rearrangement. *Journal of Adhesion* **2004**, *80* (6), 481-496.
31. Imperiali, L.; Liao, K.-H.; Clasen, C.; Fransaer, J.; Macosko, C. W.; Vermant, J. Interfacial Rheology and Structure of Tiled Graphene Oxide Sheets. *Langmuir* **2012**, *28* (21), 7990-8000.

32. Wang, J.; Opedal, N. v. d. T.; Lu, Q.; Xu, Z.; Zeng, H.; Sjoblom, J. Probing Molecular Interactions of an Asphaltene Model Compound in Organic Solvents Using a Surface Forces Apparatus (SFA). *Energy & Fuels* **2012**, *26* (5), 2591-2599.
33. Yarranton, H. W.; Masliyah, J. H. Molar mass distribution and solubility modeling of asphaltenes. *Aiche Journal* **1996**, *42* (12), 3533-3543.
34. Verruto, V. J.; Kilpatrick, P. K. Water-in-Model Oil Emulsions Studied by Small-Angle Neutron Scattering: Interfacial Film Thickness and Composition. *Langmuir* **2008**, *24* (22), 12807-12822.
35. Ivanov, I. B.; Dimitrova, D. T. Thin Film Drainage. *Thin Liquid Films Fundamentals and Applications - Surfactant Science Series* **1988**, *29*, 379-496.
36. Czarnecki, J.; Tchoukov, P.; Dabros, T. Possible Role of Asphaltenes in the Stabilization of Water-in-Crude Oil Emulsions. *Energy & Fuels* **2012**, *26* (9), 5782-5786.
37. Sarkar, J.; Sharma, A. A Unified Theory of Instabilities in Viscoelastic Thin Films: From Wetting to Confined Films, From Viscous to Elastic Films, and From Short to Long Waves. *Langmuir* **2010**, *26* (11), 8464-8473.

TOC Graphic

